APPLIED ORGANOMETALLIC CHEMISTRY
Appl. Organometal. Chem. 2003; **17**: 268–276
Published online in Wiley InterScience (www.interscience.wiley.com). DOI:10.1002/aoc.452

Characterization of aluminum–organic-stabilized platinum–colloid networks with electron and photon spectroscopies

L. Beuermann[1], W. Maus-Friedrichs[1], S. Krischok[1], V. Kempter[1], S. Bucher[2], H. Modrow[2], J. Hormes[3], N. Waldöfner[4] and H. Bönnemann[4]*

[1]Institut für Physik und Physikalische Technologien der Technischen Universität Clausthal, Leibnizstr. 4, 38678 Clausthal–Zellerfeld, Germany
[2]Physikalisches Institut der Universität Bonn, Nussallee 12, 53113 Bonn, Germany
[3]Center for Advanced Microstructures and Devices, Baton Rouge, LA 70809, USA
[4]MPI für Kohlenforschung, Kaiser-Wilhelm-Platz 1, 45 470 Mülheim an der Ruhr, Germany

Received 29 September 2002; Accepted 2 February 2003

We have measured and interpreted the ultraviolet (HeI) and X-ray photoelectron spectra and the metastable impact electron spectra (MIES) from aluminum–organic-stabilized platinum–colloids and colloid networks, deposited on silicon substrates and characterized by X-ray photoelectron spectroscopy, scanning Auger electron microscopy and transmission electron microscopy. MIES, in particular, gives information on the electronic structure of the spacer molecules interconnecting the colloids.

In addition, changes in the electronic structure of the platinum clusters that are induced by different spacer molecules were identified by means of X-ray absorption near-edge structure measurements at the platinum L_{III}-edge of these materials. This combination of techniques was also employed to follow the chemical changes that occur upon heating of the network *in situ*. It turns out that the thermal decomposition of the network is driven by the disintegration of the spacer molecules. Moreover, less sintering of the colloidal particles occurs in the networked systems than in unconnected particles. Most of the networked platinum–particles are still present in their original shape even after the destruction of spacer molecules. This observation could be linked to the encapsulation of these platinum particles into an (Al–O) protecting shell. Copyright © 2003 John Wiley & Sons, Ltd.

KEYWORDS: platinum; colloid networks; photoelectron spectroscopy; XANES; MIES; thermal decomposition

INTRODUCTION

The assembly of nanosized metal particles into highly ordered arrays has become a new trend in chemistry over the past few years.[1–3] The resulting new materials are expected to exhibit new collective properties, which could make them suitable for applications in microelectronics[4,5] or optical devices. Nanocrystal superlattices and metal colloid networks have been prepared by several groups.[6–12] However, bottom-up preparations of nanoparticles to give three—dimensional structures still remain a challenge for synthetic chemists. In our case, the platinum colloids are prepared by the reduction of platinumacetylacetonate with trimethylaluminum, which typically results in spherical platinum particles with 1 nm diameter. The key feature of this synthesis is the formation of a reactive metal–organic colloidal protecting shell (see Eqn. (1)) around the particles.[13] The reactive Al–CH_3 groups present in the protecting shell open up the possibility to substitute organic groups at the aluminum in order, for example, to modify the dispersive properties of the colloids.[14]

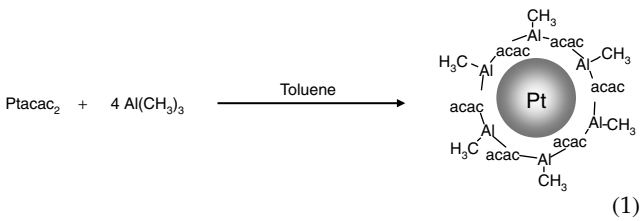

(1)

*Correspondence to: H. Bönnemann, MPI für Kohlenforschung, Kaiser-Wilhelm-Platz 1, 45 470 Mülheim an der Ruhr, Germany.
E-mail: boennemann@mpi-muelheim.mpg.de
Contract/grant sponsor: Deutsche Forschungsgemeinschaft; Contract/grant numbers: Bo 1135/3-2; Ho 887/7-2; Ke 155/34-2.

These substituents can also be bifunctional as shown Eqn. (2):

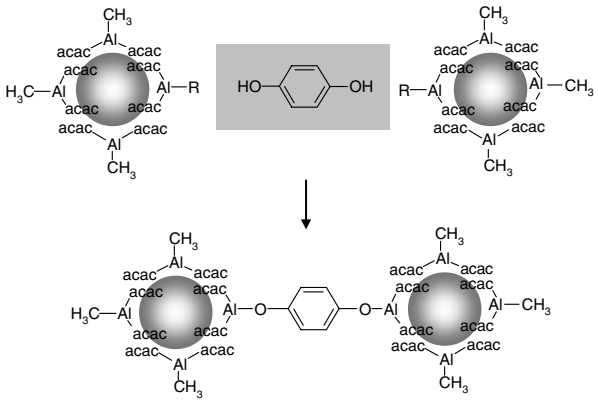

(2)

In this case a crosslinking of colloid particles can be brought about, which leads to a hybrid polymer. For example, an organic–inorganic network has been formed by reacting the colloid with bifunctional alcohols. Whereas details of the preparation pathway and the structural characterization of metal–organic hybrids formed by the crosslinking of platinum nanoparticles with bifunctional spacer molecules have been described previously,[15,16] this study is devoted to the characterization of their electronic structure and the changes induced by exposure to thermal load.

In addition to electron microscopy (scanning Auger electron microscopy (SAM) and transmission electron microscopy (TEM)) and X-ray photoelectron spectroscopy (XPS), we have investigated networks formed from aluminum–organic-stabilized platinum–colloids, deposited on silicon substrates, by ultraviolet photoelectron spectroscopy (UPS(HeI)) and metastable impact electron spectroscopy (MIES) as well as by X-ray near-edge structure (XANES) spectroscopy. By combining the above-mentioned methods we have obtained detailed information on both the platinum core of the stabilized colloids and the spacer molecules (hydroquinone, chlorohydroquinone) that stabilize the colloid network.

EXPERIMENTAL DETAILS

Preparation of colloidal platinum networks

Aluminum–organic prestabilized platinum–colloids

1.97 g (5 mmol) $Pt(acac)_2$ was dissolved under argon atmosphere in 200 ml dry toluene. 1.44 g (20 mmol) $Al(CH_3)_3$ was dissolved in 200 ml toluene and carefully added over 24 h at 40 °C. After the gas evolution had stopped, all volatile components were completely evaporated *in vacuo*. In the residue, 2.4 g colloidal platinum was obtained in the form of a black, air-sensitive powder. The platinum content of the colloid was 40%. According to protonolysis with acetic acid, six Al–CH_3 groups per platinum are present.

Modification of platinum particles with monofunctional alcohols

0.5 g of the platinum–colloid was dissolved in 500 ml dry tetrahydrofuran (THF). 0.64 g (4.97 mmol) 3-chlorophenol was dissolved in 200 ml THF and added dropwise to the colloidal solution. The evaporation of the solvent yielded 1.1 g of the modified platinum–colloid.

Crosslinking of platinum particles

0.5 g of the platinum–colloid was dissolved in 500 ml dry THF. 0.68 g (6.18 mmol) hydroquinone was dissolved in 200 ml THF and added dropwise to the colloidal solution. The colloidal network precipitated and was filtered and washed with THF. The preparation of platinum–colloid networks with chlorohydroquinone was made accordingly. In order to deposit the colloids onto silicon substrates at room temperature they were diluted in toluol in an ultrasonic bath preparation.

Experimental details of the MIES/UPS measurements

Details of the apparatus employed for the electron spectroscopic measurements can be found elsewhere.[17–19] Briefly, a cold cathode helium gas discharge source served both as the source for an intense metastable helium beam for MIES ($He^*2^3S/2^1S$) with 19.8/20.6 eV excitation energy and as an HeI photon source for UPS (HeI with 21.2 eV). The contributions to the electron spectra from metastables and photons within the beam were separated be means of a time-of-flight technique combined with a double counter system allowing one to measure MIES and UPS spectra simultaneously. The incidence angle of metastables and photons is 45° with respect to the surface; electrons emitted in the direction normal to the surface are analyzed. The energy scales in the figures are adjusted in such a way that electrons emitted from the Fermi level E_F, i.e. electrons with the maximal kinetic energy, show up at the fixed energy $E_b = 0$ eV. For photoelectrons and electrons generated in MIES in the Auger deexcitation process the E_b values are their binding energies with respect to the Fermi level. The low energy onset of the spectra directly reflects the surface work function. In the UPS(HeI) spectra E_F is positioned at 21.2 eV by choosing a suitable bias potential. With this choice, the low-energy cutoff gives the work function of the surface directly. Any changes in the position of the low-energy cutoff of the spectra reflect directly the change of the work function occurring during the deposition of the stabilized platinum–colloids or during the heating of the films (which is done under ultrahigh vacuum (UHV) conditions). For the characterization of the chemical composition of the surface and the stabilized platinum films the apparatus is equipped with a twin anode (Mg/Al) XPS source. TEM measurements were perfomed on a Siemens Elmiskop 102 (100 kV acceleration voltage). To prepare the samples for these measurements, a small amount of the sample was suspended in toluene in an ultrasonic bath and placed on a carbon-coated copper grid (400 mesh per inch).

The identification of the spectral structures observed in the MIES and UPS spectra was made on the following basis.

(1) Features due to the ionization of the σ and π molecular orbitals (MOs) of the aromatic rings of the spacer molecules can be related to the corresponding features in the MIES and UPS spectra of the trimer of the 2,4,6-tris-(*p*-cumylphenylcyanate)-1,3,5-triazine (*p*-CPC) trimer molecules deposited onto silicon substrates.[17,20] This comparison appears justified because, apart from the cores of the two molecular structures (a triazine ring in the case of *p*-CPC and platinum–colloids in the present cases), the ligand's geometrical structure, consisting of phenyl rings, is similar in both cases.

Some information on the electronic structure of the aluminum–organic prestabilized colloids can also be derived from our MIES/UPS study on benzene adsorbed on molybdenum substrates.[21]

(2) The identification of spectral features, related to the presence of the chlorine atom in the spacer molecules, is made in the following way: we consult available MIES spectra of chlorine-containing organic molecules, in particular chlorobenzylmercaptan (CBM) on Au(111) substrates[22] and chloroaluminum phthalocyanine (ClAlPc).[23] From these results we conclude that a comparatively well-localized spectral feature from the ionization of the Cl(3p) is expected in the MIES spectra around $E_b = 6$ eV (with respect to the Fermi level)[22] provided that the He^*-probe atom employed for MIES can interact with the charge cloud of the chlorine atom. In this case electron emission induced by the Auger deexcitation process, involving the Cl(3p) and He(1s) states, will occur.

(3) Features originating from an eventual (Al–O) network encapsulating the platinum–colloids after heating the platinum films can be identified by a comparison with MIES/UPS spectra from (Mg–O) and (Al–O) films on metallic substrates[18,24] and silicon.[25]

Experimental details of the XANES measurements

X-ray absorption measurements were performed on beamline BN3 of the Electron Stretcher and Accelerator ELSA at Bonn University. The setup of this beamline is described elsewhere in detail.[26] For the measurements, ELSA was operated at an electron energy of 2.7 GeV and an average electron current of 35 mA. The synchrotron radiation from ELSA was monochromatized with Si(400) crystals, which yield a step width of about 0.94 eV at the platinum L_{111}-edge (11 564 eV). The spectra at this edge were taken with argon in the ionization chambers at a pressure of 500 mbar.

The photon energy was scanned from 11 500 to 11 700 eV. For each data point, an integration time of 500 ms was used. To prepare the samples for measurement, the dried colloids were mixed with boron nitride and pressed to pellets. The optimal sample thickness was found by trial and error and was chosen in such a way that the maximum absorption μd was not higher than 1.2. The entire process of sample preparation was done in a glove box filled with argon. Sample transfer to the measurement station also took place under inert gas atmosphere. To compare the different measurements, the experimental data were evaluated in the following way. After subtraction of a linear background, which is fitted in the pre-edge region, the absorption edge was normalized to unity by dividing through the absorption μd at an energy of 11 633.9 eV, representing an inflection point of a shape resonance of the metal foil. Photon energy calibration was made in relation to the pure metal: the first inflection point was set to the binding energy of the $2p_{3/2}$ electron, 11 564 eV.

RESULTS

MIES and UPS results

Figure 1 shows TEM images of the free platinum–colloids (a) and the network formed after the crosslinking of the

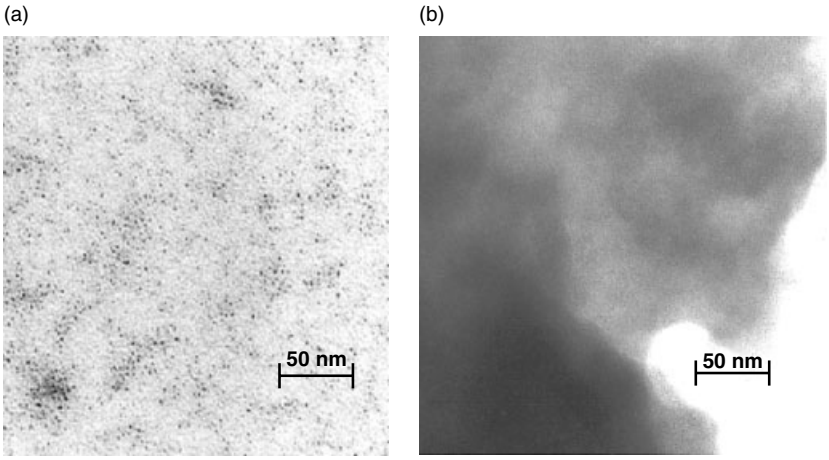

Figure 1. TEM images of the free platinum–colloids (a) and the network formed after the crosslinking the platinum colloids with hydroquinone spacer molecules (b).

platinum–colloids with hydroquinone spacer molecules (b). Fig. 1a displays a narrow particle size distribution (mean particle size: 1.2 nm). The crosslinked product (Fig. 1b) exhibits a very dense colloid network with a uniform interparticle distance. In addition, certain regions of the image show a parallel alignment of the particles, which may be attributed to ordered structures.

The XPS spectra of the samples studied by MIES and UPS (i.e. after diluting the sample studied in Fig. 1 in toluol and the deposition of the dilution on the silicon substrate) establish the presence of chlorine in platinum–colloids crosslinked by chlorohydroquinone spacers. Emission from both the silicon substrate and the platinum–colloids is present in all spectra. We also see the emission from the aluminum anchor molecules to which the spacer molecules are tied. SAM indicates that the effect of the dilution is the formation of micrometer-sized platinum–colloid aggregates. The main effect of the heating procedure is the disappearance of the chlorine in the spectra and an increase of the emission from platinum and the silicon substrate. The C1s and O1s intensities are not affected much by the heating procedure, indicating that, although the spacer molecules may become destroyed, their constituents remain in the film structure.

Figure 2 presents MIES and UPS(HeI) spectra for platinum–colloids crosslinked by hydroquinone spacers. Figure 3a and b show the spectral changes of these spectra taking place when heating the film under UHV

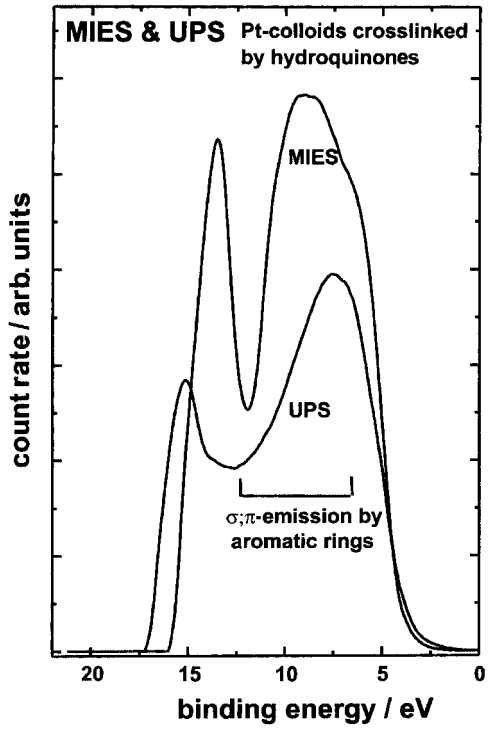

Figure 2. MIES and UPS(HeI) spectra for aluminum–organic-stabilized platinum–colloids crosslinked by hydroquinone spacers after dilution onto silica substrates.

conditions. Figure 4 displays MIES and UPS spectra for platinum–colloids crosslinked by chlorohydroquinone spacers; when heating, results similar to those of Fig. 3 are obtained. MIES/UPS results (not shown) obtained from platinum–colloids modified (but not crosslinked) by 3-chlorophenol molecules are rather similar to those of Figs 2 and 3 for platinum–colloids crosslinked with hydroquinone spacers. MIES results obtained with phenol films (not shown) confirm that the structure observed between 5 and 7 eV is not caused by oxygen or carbon contamination.

For the as-prepared films there is practically no emission for binding energies E_b smaller than 3.5 eV. Together with the fact that the work function of the as-prepared films is 4 eV (as estimated from the low-energy onset of the MIES spectra), we conclude that the films studied possess insulating character, featuring a band gap of 7.5 eV. The procedure to determine the insulator band gap width from the position of the valence band maximum with respect to E_F and the work function of the sample is described elsewhere.[19] We do not interpret the MIES/UPS spectra for $E_b > 11.5$ eV because this range of binding energies is strongly affected by contributions from secondary and backscattered electrons. Upon heating, intensity appears in the band gap, i.e. between the Fermi energy and about 4 eV. This indicates that the film adopts metallic properties. The coarse structure of the MIES spectra for both networks resembles that displayed by *p*-CPC films on silicon.[17,20] In both cases, the part of the emission that can be attributed to the organic components of the films studied, *p*-CPC on the one hand and the stabilized platinum–colloids on the other hand, is largely confined to the energy range between $E_b = 4$ to 12 eV. The onset of this emission takes place near $E_b = 3.5$ eV and terminates rather abruptly near $E_b = 11.5$ eV. Whereas the MIES/UPS spectra from *p*-CPC show rather well-resolved fine structure, due to the ionization of, in particular, the π MOs of the aromatic rings, the present spectra show at most indications of a fine structure. From this comparison we conclude that the emission between 4 and 11 eV is largely due to the ionization of the π and σ MOs of the aromatic rings in the spacers. In particular, the emission between 4 and about 8 eV is largely due to the ionization of the π MOs. Apparently, as inspection of Figs 2 and 4 shows, the main effect of the chlorination of the spacer molecules is a reduction of the emission in the range between 4 and 8 eV, i.e. a reduction in the emission from the ionization of the π MOs. In addition, we see some fine structure in the MIES spectra in the range $E_b = 3$ to 7 eV, which, as the comparison with the MIES results for 4(2)-CBM suggests,[22] must be attributed to the ionization of the Cl(3p) orbitals. The two shoulders correspond to the structures A and B in Ref. [22] and are thought to correspond to the ionization of the π orbitals of chlorine, and of the non-bonding chlorine orbitals both parallel and perpendicular to the plane of the molecule.[22]

Upon heating, the emission from the aromatic rings disappears in the MIES spectra. On the other hand, the XPS spectra indicate that the organic fragments originating from

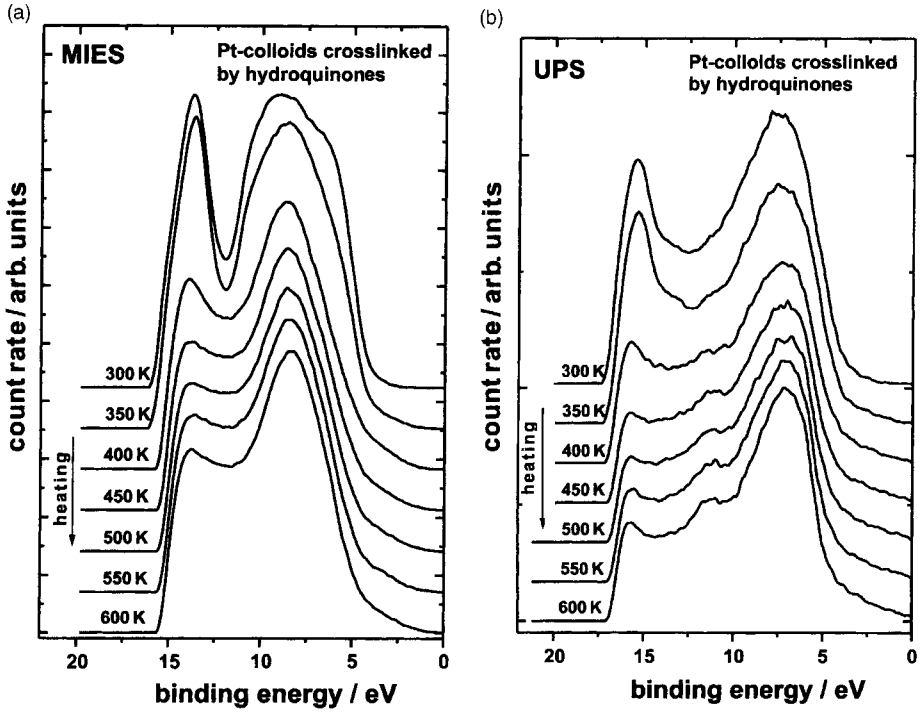

Figure 3. Changes in the MIES (a) and UPS (b) spectra of Fig. 2 as a function of the substrate temperature.

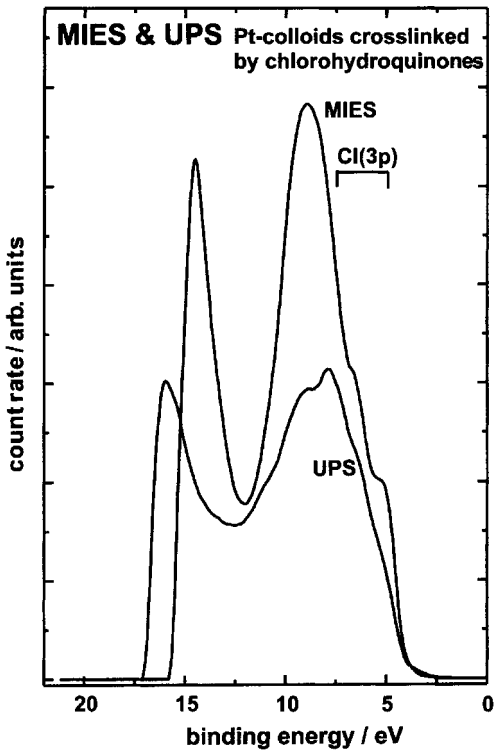

Figure 4. Same as Fig. 2, but with chlorohydroquinone spacers.

the heating procedure remain in the film. As a consequence of the heating, the spectra become similar to those found from oxide films on metallic and silicon substrates, (Mg–O) and (Al–O) in particular.[18,24,25]

XANES results

Figure 5 displays the edge region of the platinum L_{III} XANES spectra of the differently modified and/or networked platinum colloids measured at three different temperatures. Clear changes in shape, position and intensity of the maximum of absorption are visible.

These differences in the spectra reflect directly changes in the electronic structure of the platinum core. As the platinum L_{III} XANES spectrum probes mainly the unoccupied density of states of platinum d-states, an increased intensity of the white line usually indicates that the electronegativity of the surroundings has increased.[27] In the case of the aluminum–organic prestabilized platinum–colloids investigated in this study, two effects have to be considered that may cause changes in the electronic structure: a possible variation of the particle size, especially during the heating process (but at least in principle also during the crosslinking process), as well as the possible electronic influence of the connecting spacer molecule, which induces changes in the surfactant shell. Whereas both effects influence shape and intensity of the white line,[28–30] the actual intensity of the shape resonances typical for platinum metal allows a rough qualitative estimate of the particle size and degree of ordering present in the sample, and thus the isolation of size effect and chemical environment on the density of states measured on the colloid. Figure 6 shows the observed post-edge structures for the varying spacer molecules at different temperatures in

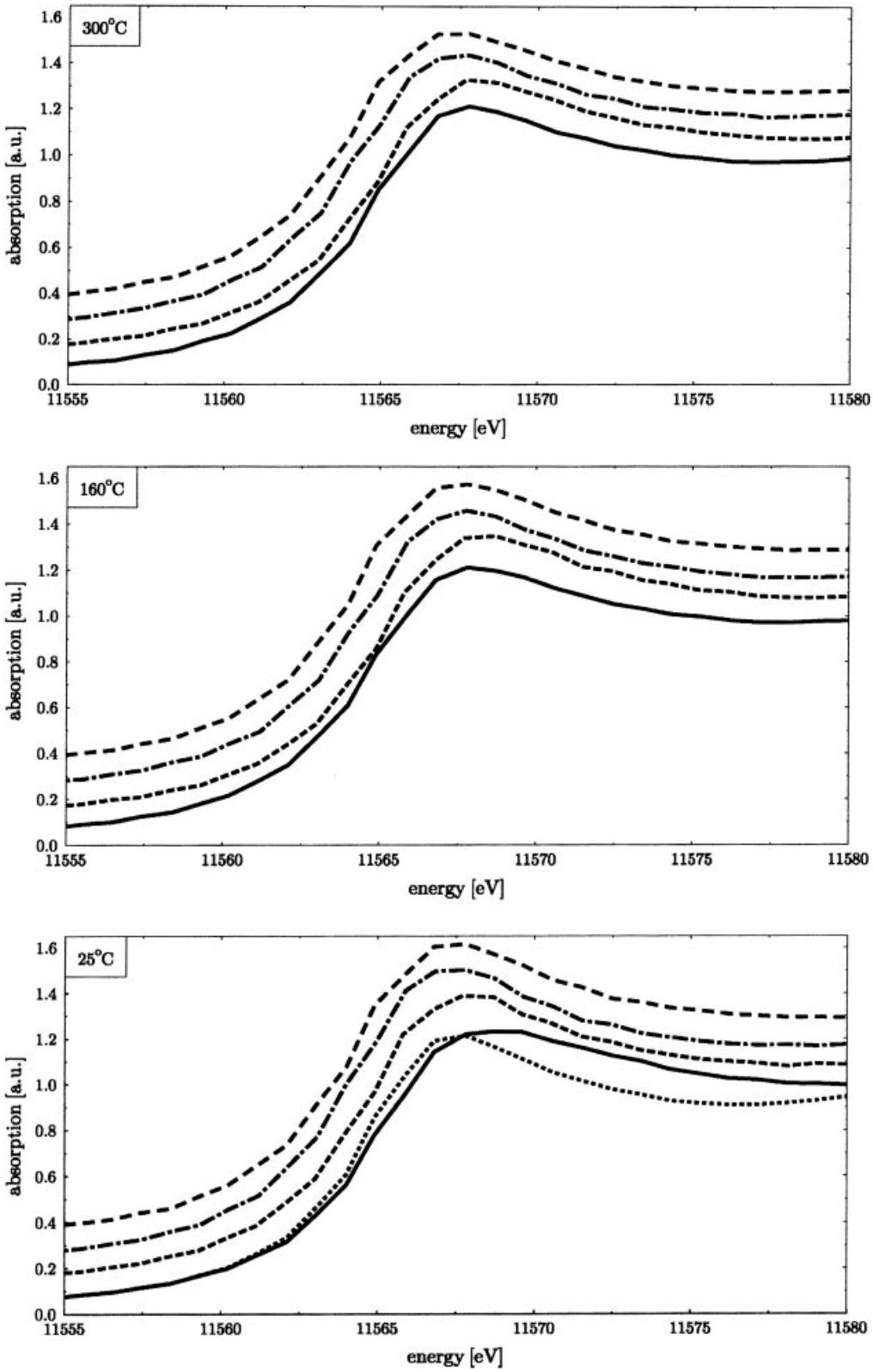

Figure 5. Changes in the platinum L_{III}-XANES spectra of non-modified (solid line), chlorophenol-modified (dash and dot), hydroquinone crosslinked (short dash) and chlorohydroquinone crosslinked (long dash) aluminum–organic-stabilized platinum–colloids at 300 °C (top), 160 °C (middle), 25 °C (bottom). For comparison, in the lowest panel a bulk platinum spectrum is also displayed (dots).

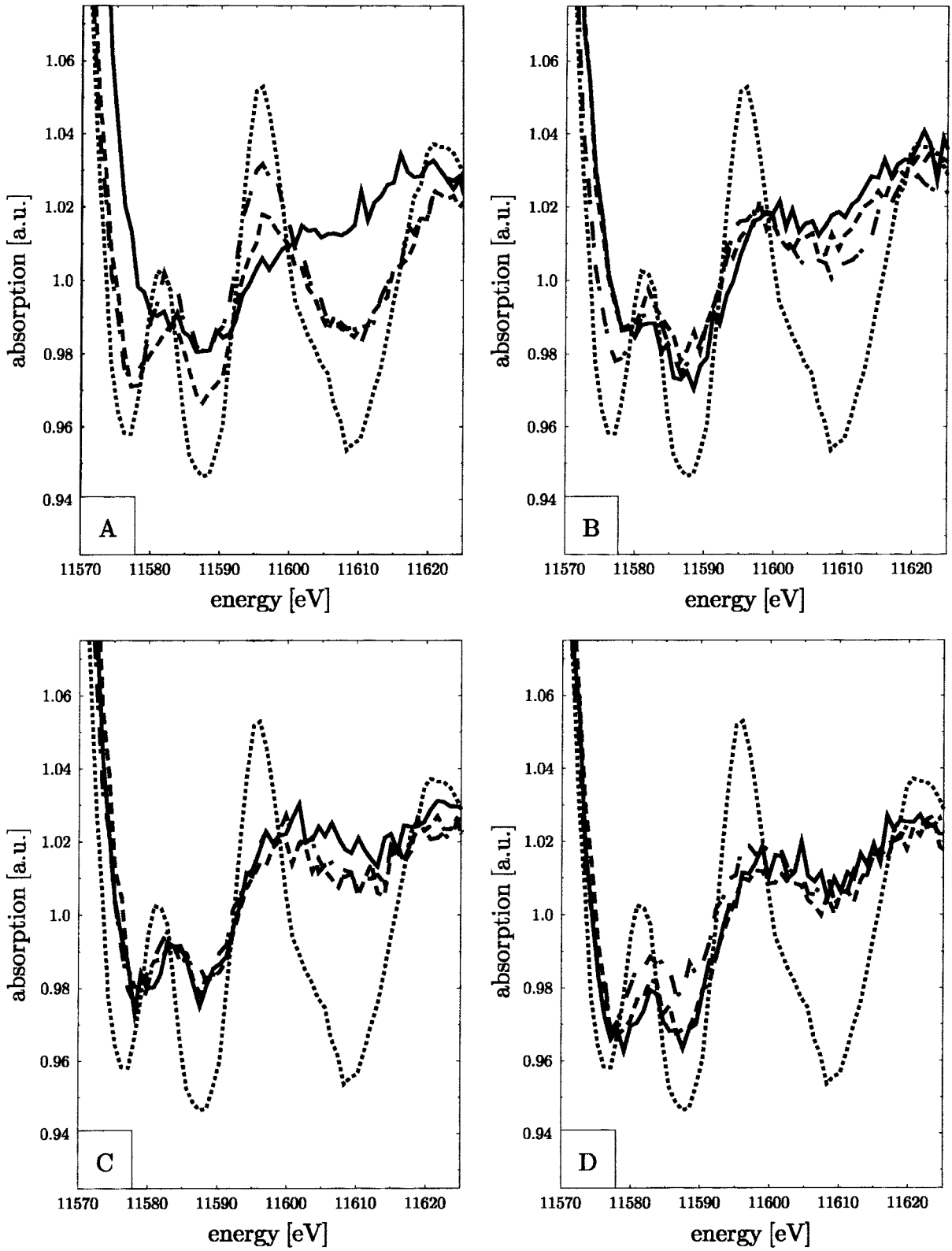

Figure 6. Temperature-dependent development of the shape resonances in the platinum L_{III}-XANES spectra of non-modified (A), chlorophenol-modified (B), hydroquinone crosslinked (C) and chlorohydroquinone crosslinked (D) aluminum–organic-stabilized platinum–colloids at 300 °C (dot), 160 °C (dash), 25 °C (solid line). For comparison, in the each panel a bulk platinum spectrum is also displayed (dash and dot).

comparison with the corresponding structures in the XANES spectrum of bulk fcc platinum.

Only for the unmodified colloid (Fig. 6A) does one observe a significant increase in the intensity of the shape resonances with temperature. This proves that the observed temperature-dependent changes in the electronic structure shown in Fig. 5 are predominantly due to changes in the surfactant shell of the colloidal particles.

It should be noted that the visual impression that the edge position seems to shift to lower energies after the modification and/or connection of the platinum–colloid, compared with the non-modified platinum–colloid, that one obtains from Fig. 5 is not supported by the experimental data. The energy position of the first inflection point of the absorption edge is 11 654 eV for all compounds. A second investigation applying the integration method[31] shows small variations of the edge position up to about 1 eV between both the non-modified and the modified the crosslinked platinum–colloids; but, because the step size between two data points is of about the same size, one can draw no conclusions from these variations and the formal valency of the platinum in all samples is zero. Still, the variation of the white line shape and intensity indicates a change of the electronic structure with the modification and the linking of the platinum–colloids by spacers.

DISCUSSION

MIES is apparently sensitive in two ways to structural changes that are introduced into the spacers by the substitution of chlorine.

(1) Chlorination leads to a remarkable reduction in the π-emission from the chlorohydroquinone rings (for $E_b = 4$ to 8 eV). This can probably be understood when assuming that the introduction of chlorine leads to the reorientation of the plane of the spacer molecules with respect to the silicon surface in such a manner that the helium probe atoms can interact less efficiently with the π MOs of the aromatic rings.

(2) Emission from the ionization of the Cl(3p) orbital is seen at $E_b = 5$ to 7 eV. This indicates that the He(1s) orbital of the helium probe atom employed for MIES overlaps with the Cl(3p) orbital of the substituted chlorine atom located in the spacer chain.

We find that the emission from the spacer molecules is much less structured than the corresponding emission from the ligand molecules in surface-adsorbed *p*-CPC molecules. One possible reason could be poorly ordered structures in the present situation, whereas in the case of *p*-CPC all the ligand molecules will be oriented more or less parallel to the substrate surface. The similarity of the results for platinum–colloids modified by 3-chlorophenol with those of Figs 2 and 4 is possibly due to the fact that in both cases the spectra are dominated by contributions from the phenyl rings. Obviously, in the case of platinum–colloids modified by 3-chlorophenol, in contrast to the sample crosslinked with chlorohydroquinone spacers, the chlorine atom is not accessible to interaction with the helium probe atom employed in MIES. When heating the colloid film, MIES witnesses the disappearence of the π-emission from the rings of the spacer molecules between $E_b = 4$ and 8 eV. XPS, on the other hand, does only give a small, unspecific change in the C(1s) and O(1s) intensities. This suggests the destruction of the spacer molecules (above 350 K).

Upon heating, intensity develops at the Fermi level in the MIES spectra. This indicates that the platinum–colloids (featuring metallic properties) become accessible to the He^*-probe atoms utilized for MIES. On the other hand, the MIES spectra between $E_b = 5$ and 10 eV resemble more and more those from metal oxide films, MgO[18] and Al_2O_3[24] in particular. This becomes understandable when one assumes that, as a consequence of the heating procedure, the platinum–colloids are surrounded by some sort of (Al–O) network. Following this tentative interpretation, most of the emission between $E_F = 5$ and 10 eV after heating would then be due to the ionization of O(2p) orbitals from oxygen atoms of the (Al–O) network.

The clear differences between the platinum L_{III} XANES spectra of the investigated materials at room temperature (Fig. 5c) demonstrate a significant influence of the surfactant shell on the electronic properties of the metallic core. This influence is already evident when comparing the spectra of the non-modified colloidal platinum particles and bulk platinum: On the high-energy side of the white line the nanoparticles show a broad shoulder, which can be explained by the presence of surface or interface states on the outer shell of the colloidal particle that contribute to the density of states at a different energy than platinum bulk states.[32] Naturally, the location of these states in the spectrum is a function of the respective interface, and thus dependent on the surfactant shell. During the process of modification and crosslinking of the colloids, at least one methyl group per aluminum atom is replaced by an O–R group. This should cause a charge transfer from aluminum to oxygen, leaving the direct environment of the metal core with a higher electron affinity, which is directly reflected in the higher intensity of the white line of these particles. The observed differences within the modified/networked particles are correlated with the presence of chlorine, which leads to an even higher depletion of charge from the metal core due to its high electron affinity and goes along with another shift in the energy position of these states. Thus, we obtain the result that the exact nature of the surfactant shell and slight modifications thereof can influence the electronic properties of the metal core of the nanoparticle considerably. A similar result has been obtained recently for $N(alkyl)_4Cl$-stabilized palladium nanoparticles.[26] Bearing in mind the considerable degree of reactivity of the aluminum–organic protection shell, which allows for a wide range of possible modifications, an improved understanding of the mechanisms of this influence might lead to novel ways to tune the electronic properties of the core selectively.

Let us turn now to the discussion of the heating process. As discussed in the MIES section above, the thermal load leads

to the destruction of the spacer molecules. This sequential destruction can also be followed in the platinum L_{III} XANES spectra, as the changes in the electronic structure that result from the process of crosslinking and modification are slowly reversed, as seen from the reduction of the white line's intensity and the changes in the shape of the white line. Still, in contrast to the non-modified particles, no significant formation of shape resonances is observed (see Fig. 6). If this was the result of an ordering process within the metal core, it should occur for all materials under investigation. In contrast to that, it is rather intuitive that both introduction of a spacer or a rigid modifying molecule should reduce agglomeration considerably. Consequently, the increasing intensity of the shape resonances in the non-modified particle can be assigned to effective enlargement of the particles due to agglomeration. The fact that this process is not even observed after the destruction of the spacer molecules supports the formation of an Al–O protecting shell that was assumed above based on the MIES data.

SUMMARY

Combining information from TEM measurements, photoelectron spectroscopies (UPS(HeI), SAM, XPS), MIES and platinum L_{III} XANES, we have gained insight into the electronic structures of aluminum–organic-stabilized free, modified and crosslinked platinum–colloids and their changes upon heating. At room temperature, significant differences between the electronic structure of aluminum–organic prestabilized platinum–colloid and the different modified/crosslinked platinum–colloids are observed. This rather unexpected result implies the possibility of influencing the electronic properties of such particles via modification of their protection shell and underlines the importance of the surfactant shell for particle properties. Also, it was possible to analyze further subtle changes in the protection shell. Although the platinum–colloid modified with 3-chlorophenol and the same colloid connected with chlorohydroquinone differ only in the additional cluster located on the second end of the spacer molecule, the chlorine can only be detected by MIES in the latter case, indicating different equilibrium positions of this molecule. The thermal load on the network leads to a disintegration of the spacer molecules, which could be followed in both MIES and XANES spectra. A clear trend towards the formation of shape resonances under thermal load is observed only for the unmodified particles, which indicates that it is driven by agglomeration, not just structural reordering within the colloidal metal cores. Interestingly, this agglomeration does not occur easily for particles that were initially surrounded by spacer molecules, even after this molecule is destroyed. Using MIES, it was possible to correlate this observation to a suggested formation of an (Al–O) protecting shell.

Acknowledgements

Financial support of the Deutsche Forschungsgemeinschaft within the SPP 1072 (grant nos: Bo 1135/3-2, Ho 887/7-2 and Ke 155/34-2) is gratefully acknowledged.

REFERENCES

1. Reetz MT, Winter M, Tesche B. *Chem. Commun.* 1997; 147.
2. Sato T, Brown D, Johnson BFG. *Chem. Commun.* 1997; 1007.
3. Schmid G, Bäumle M, Beyer N. *Angew. Chem. Int. Ed. Engl.* 2000; **39**: 182.
4. Schön G, Simon U. *Colloid Polym. Sci.* 1995; **273**: 101.
5. Schön G, Simon U. *Colloid Polym. Sci.* 1995; **273**: 202.
6. Taleb A, Petit C, Pileni MP. *Chem. Mater.* 1997; **9**: 950.
7. Motte L, Billoudet F, Lacaze E, Doulin J, Pileni MP. *J. Phys. Chem. B* 1997; **101**: 138.
8. Lin XM, Sorensen CM, Klabunde KJ. *Chem. Mater.* 1999; **11**: 198.
9. Brust M, Bethell D, Schiffrin DJ, Kiely CJ. *Adv. Mater.* 1995; **7**(9): 795.
10. Shenton W, Davis SA, Mann S. *Adv. Mater* 1999; **11**(6): 449.
11. Connolly S, Fitzmaurice D. *Adv. Mater* 1999; **11**(14): 1202.
12. Korgel BA, Fullam S, Connolly S, Fitzmaurice D. *J. Phys. Chem. B* 1998; **102**: 8379.
13. Bönnemann H, Brijoux W, Brinkmann R, Endruschat U, Hofstadt W, Angermund K. *Rev. Roum. Chim.* 1999; 1003.
14. Bönnemann H, Brijoux W, Brinkmann R. (Studiengesellschaft Kohle mbH, DE). *German Patent* DE19821968 A, 1999.
15. Bönnemann H, Waldöfner N, Haubold HG, Vad T. *Chem. Mater.* 2002; **14**: 1115.
16. Vad T, Haubold HG, Waldöfner N, Bönnemann H. *J. Appl. Crystallogr.* 2002; **35**: 459.
17. Dieckhoff S, Schlett V, Possart W, Hennemann O-D, Günster J, Kempter V. *Appl. Surf. Sci.* 1996; **103**: 221.
18. Ochs D, Brause M, Maus-Friedrichs W, Kempter V, Puchin V, Shluger A, Kantorovich L. *Surf. Sci.* 1996; **365**: 557.
19. Kantorovich L, Shluger AL, Sushko PV, Günster J, Stracke P, Goodman DW, Kempter V. *Faraday Discuss* 1999; **114**: 173.
20. Dieckhoff S, Höper R, Schlett V, Gesang T, Possart W, Hennemann O-D, Günster J, Kempter V. *Fresenius J. Anal. Chem.* 1997; **358**: 258.
21. Günster J, Liu G, Kempter V, Goodman DW. *Surf. Sci.* 1999; **415**: 303.
22. Stultz J, Krischok S, Goodman DW. *Langmuir* 2002; **18**: 2962.
23. Pasinski T, Aoki M, Masuda S, Harada Y, Ueno N, Hoshi H, Maruyama Y. *J. Phys. Chem.* 1995; **99**: 12 858.
24. Puchin VE, Gale JD, Shluger AL, Kotomin EA, Günster J, Brause M, Kempter V. *Surf. Sci.* 1997; **370**: 190.
25. Ochs D, Brause M, Maus-Friedrichs W, Kempter V. *J. Electron Spectrosc. Relat. Phenom.* 1998; **88–91**: 725.
26. Bucher S, Hormes J, Modrow H, Brinkmann R, Waldöfner N, Bönnemann H, Beuermann L, Krischok S, Maus-Friedrichs W, Kempter V. *Surf. Sci.* 2002; **497**: 321.
27. Rehr JJ, Ankudinov AL, Bare SR, Low J. *J. Synchrotron Radiat.* 2001; **8**: 547.
28. Bazin D, Sayers D, Rehr JJ, Mottet C. *J. Phys. Chem. B* 1997; **101**: 5332.
29. Bazin D, Sayers D, Rehr JJ. *J. Phys. Chem. B* 1997; **101**: 11 040.
30. Rothe J, Köhl G, Hormes J, Bönnemann H, Brijoux W, Siepen K. *J. Phys. IV* 1997; **7**(C2): 959.
31. Capehart TW, Herbst JF, Mishra RK, Pinkerton FE. *Phys. Rev. B* 1995; **52**: 7907.
32. Bitter JH, Oudenhuizen M, Cauqui M, Bearnal S, Koningsberger D. In XAFS XI, Ako, 2000.

